AIAA JOURNAL
Vol. 32, No. 5, May 1994

Structural Damage Detection of Space Truss Structures Using Best Achievable Eigenvectors

Tae W. Lim*
University of Kansas, Lawrence, Kansas 66047
and
Thomas A. L. Kashangaki†
NASA Langley Research Center, Hampton, Virginia 23681

A method is presented by which measured modes and frequencies from a modal test can be used to determine the location and magnitude of damage in a space truss structure. The damage is located by computing the Euclidean distances between the measured mode shapes and the best achievable eigenvectors. The best achievable eigenvectors are the projection of the measured mode shapes onto the subspace defined by the refined analytical model of the structure and the measured frequencies. Loss of both stiffness and mass properties can be located and quantified. To examine the performance of the method when experimentally measured modes are employed, various damage detection studies using a laboratory eight-bay truss structure were conducted. The method performs well even though the measurement errors inevitably make the damage location more difficult.

Introduction

FUTURE structures in space will be orders of magnitude larger and more complex than their predecessors. Structures such as Space Station Freedom will typically be built around a large flexible frame and consist of habitation and experiment modules, flexible and articulating appendages, and numerous utility trays and payloads. Along with the need to design the spacecraft to be lightweight, strong, and modular for ease of expansion, repair, and modification, the complexity and size of these structures require that the integrity of the structures be monitored periodically.

Several researchers have studied the possibility of detecting damage or structural anomalies to large space trusses and locating the site of this damage based on changes in the natural frequencies and mode shapes of the structures. References 1 and 2 provide a comprehensive overview of many of the proposed methods in this respect and the issues involved with on-orbit modal identification and structural verification. There are several distinct classes of model improvement/damage location methods. Each of these methods begins with an initial finite element representation of the structure. In the case of model improvement, the goal is to use test data of the actual structure to modify this initial finite element model so that it may serve as an accurate representation of the undamaged structure. In the case of damage location, the goal is to use test data from the damaged structure and the updated/correlated finite element model of the undamaged structure to determine changes to the stiffness and/or mass matrices that would account for the observed differences in the measured modes and frequencies.

The class of update methods that has been explored most widely is known as optimal matrix modification. The goal of the optimal matrix modification is to find an updated matrix (stiffness and/or mass) that is as close as possible to the original matrix (assumed to be almost correct) that accurately produces the measured modes and frequencies. Brock[3] introduced the framework that has been used in these methods in 1968. Baruch[4] and Berman and Nagy[5] followed with update methods based on Brock's work. Kabe[6] was the first to develop a method that imposed a constraint on permissible load paths, greatly improving the performance in obtaining physically realizable matrix updates. Smith and Hendricks[7] used Kabe's method to develop a strategy for on-orbit damage location in truss structures. Kammer[8] later reformulated and improved on the computational efficiency of Kabe's method. Smith and Beattie[9] introduced a class of secant method updates and showed that many of the previously referenced methods could be cast in this way. These new developments have improved the usefulness of optimal update methods to the point where they can be considered viable tools for practical model improvement and damage location.

Sensitivity-based update methods have been widely used in industry for performing test/analysis correlation and finite element model improvement. These methods start with the derivatives of the eigenvalue and/or eigenvectors to changes in material and physical parameters. These sensitivity coefficients are then used to calculate changes in the parameters that would force the analysis frequencies and modes to match those measured in a test.[10] Various optimization techniques can be used to converge on near-optimal solutions. Sensitivity-based update methods have been incorporated in several commercially available analysis tools such as MSC/NASTRAN.[11] These methods generally require considerable computational expense.

The newest class of model improvement/damage location methods are those based on eigenstructure assignment techniques. Control system designers have traditionally used such techniques to force a structure to respond in a predetermined way. That is, the eigenstructure—eigenvalues and eigenvectors—of the structure can be tailored to suit a given purpose. Andry et al.[12] present an excellent overview of eigenstructure assignment theory and applications. For model improvement and damage location, the desired eigenstructure is the one that is measured in the test. Inman and Minas[13] and Zimmerman and Widengren[14] have derived methods that determine the pseudo (fictitious) controller which would be required to produce the test data. The control gains and forces can then be translated into matrix adjustments applied to the initial finite element model. However, these methods are formulated in terms of control systems theory and may not be directly useful to the structural dynamicist. Zimmerman and Kaouk present a method[15] which is similar in concept to the method presented in this paper. In order to locate the damaged structural element, Zim-

Received April 21, 1993; revision received Oct. 25, 1993; accepted for publication Oct. 25, 1993.

*Assistant Professor, Department of Aerospace Engineering. Member AIAA.
†Aerospace Engineer, Spacecraft Dynamics Branch. Member AIAA.

merman and Kaouk's method identifies matrix coefficient changes due to damage and thus requires an additional step of identifying structural members corresponding to the changes. This additional step will not be straightforward for complicated structures because several structural members can contribute to the stiffness coefficient change at a given degree of freedom (DOF).

In this paper, using the concept of best achievable eigenvectors, a method is developed by which measured modes and frequencies can be used to determine both the location and magnitude of damage in truss structures. Instead of identifying matrix coefficient changes, this method identifies directly damaged structural elements. Thus, the additional step of identifying damaged members from the matrix coefficient changes is avoided. In the theoretical development that follows, damage is assumed to be due to the loss of stiffness and, in some cases, the loss of mass, of one or more members. It is assumed that the damping characteristics of the structure are not affected due to damage. Thus, damping terms are ignored in the development. To deal with the measurement error of modal test data, a concept of filtering test mode shapes using the refined analytical model and test frequencies is presented. To evaluate the capability of the method and to demonstrate the damage detection procedure, the method is applied to damage detection of a laboratory eight-bay space truss structure with measured test data.

Theoretical Development

The equations of motion for an n-DOF structural dynamic system can be expressed as

$$\boldsymbol{M}\ddot{\boldsymbol{x}} + \boldsymbol{K}\boldsymbol{x} = \boldsymbol{f}(t) \tag{1}$$

where $\boldsymbol{M}$ and $\boldsymbol{K}$ are $n \times n$ system mass and stiffness matrices, respectively, and $\boldsymbol{x}$ and $\boldsymbol{f}(t)$ are $n \times 1$ physical displacement and applied load vectors, respectively. The eigenvalue equation associated with Eq. (1) is

$$\boldsymbol{K}\Phi = \boldsymbol{M}\Phi\Lambda \tag{2}$$

where Φ is an $n \times r$ system modal matrix containing r mode shapes and Λ is a diagonal matrix containing r system eigenvalues. The system stiffness and mass matrices can be represented as a sum of the element stiffness and mass matrices, respectively,

$$\boldsymbol{K} = \sum_{i=1}^{p} \boldsymbol{K}_i \tag{3}$$

$$\boldsymbol{M} = \sum_{i=1}^{q} \boldsymbol{M}_i \tag{4}$$

where $\boldsymbol{K}_i$ and $\boldsymbol{M}_i$ are the element stiffness and mass matrices and p and q are the total number of stiffness and mass element matrices, respectively.

When damage has occurred in the structure, the system matrices of the damaged structure can be represented as the sum of the original system matrices and each of the element matrices multiplied by a reduction factor

$$\boldsymbol{K}_d = \boldsymbol{K}_u + \sum_{i=1}^{p} a_i \boldsymbol{K}_i \tag{5}$$

$$\boldsymbol{M}_d = \boldsymbol{M}_u + \sum_{i=1}^{q} b_i \boldsymbol{M}_i \tag{6}$$

where $\boldsymbol{K}_d$ and $\boldsymbol{M}_d$ are the stiffness and mass matrices of the damaged structure, $\boldsymbol{K}_u$ and $\boldsymbol{M}_u$ are the stiffness and mass matrices of the undamaged structure, and a_i and b_i are the ith stiffness and mass reduction factors, respectively. Let a_k and b_k correspond to element k. If element k is undamaged, both have values of zero. If element k has been completely removed then have a_k and b_k values of -1. Values in between represent partial damage to the member. Note that a_k and b_k do not have to be equal. In fact, a member can lose all of its load-carrying capacity but retain most of its mass. In addition, there may be some large masses on a structure that do not contribute to the stiffness or load path and are modeled simply as lumped masses. Loss of such a member does not detract from the stiffness matrix but could represent a substantial loss from the system mass matrix.

Identification of the Location of Damage

Assume that a modal survey was performed on a damaged structure and r number of modes were found to be changed due to damage. Substitute Eqs. (5) and (6) into the eigenvalue equation, Eq. (2), along with the r number of test modes of the damaged structure. Rearrange to obtain

$$\sum_{i=1}^{p} a_i \boldsymbol{K}_i \Phi_t - \sum_{i=1}^{q} b_i \boldsymbol{M}_i \Phi_t \Lambda_t = \boldsymbol{M}_u \Phi_t \Lambda_t - \boldsymbol{K}_u \Phi_t \tag{7}$$

where the subscript t is used to denote the quantities obtained from the test. Typically, the test mode shapes are available only at the test DOFs where the transducers are placed for a modal test. In this case, eigenvector expansion algorithms[5,16] can be employed to expand the mode shapes from the test DOFs to the finite element DOFs. In this paper, it is assumed that the mode shapes at the finite element DOFs have been made available either by expanding the mode shapes at the test DOFs or by measuring the entire finite element DOFs. For the jth test mode, the preceding equation can be rewritten as

$$\sum_{i=1}^{p} a_i \boldsymbol{E}_j^{-1} \boldsymbol{K}_i \phi_{tj} - \sum_{i=1}^{q} b_i \omega_{tj}^2 \boldsymbol{E}_j^{-1} \boldsymbol{M}_i \phi_{tj} = \phi_{tj} \tag{8}$$

where

$$\boldsymbol{E}_j = (\omega_{tj}^2 \boldsymbol{M}_u - \boldsymbol{K}_u) \tag{9}$$

The quantities ω_{tj} and ϕ_{tj} are the measured jth natural frequency and mode shape of the damaged structure, respectively. Note that $\boldsymbol{E}_j^{-1}$ exists since $\omega_{tj} \neq \omega_j$ due to damage. When the frequency change due to damage is small, i.e., $\omega_{tj} \approx \omega_j$, the matrix $\boldsymbol{E}_j$ can be ill-conditioned. Therefore, even for the perfect modal test data, the smallest damage that can be detected is limited by the numerical conditioning of $\boldsymbol{E}_j$. Among the test modes that can be used for damage detection, the modes corresponding to the smallest condition number of $\boldsymbol{E}_j$ should be employed to improve the numerical performance of the method. Define the following matrices

$$\boldsymbol{A}_{ij} = \boldsymbol{E}_j^{-1} \boldsymbol{K}_i \tag{10}$$

$$\boldsymbol{B}_{ij} = -\omega_{tj}^2 \boldsymbol{E}_j^{-1} \boldsymbol{M}_i \tag{11}$$

Equation (8) can now be expressed as

$$\sum_{i=1}^{p} a_i \boldsymbol{A}_{ij} \phi_{tj} + \sum_{i=1}^{q} b_i \boldsymbol{B}_{ij} \phi_{tj} = \phi_{tj} \tag{12}$$

Define a vector containing the reduction factors as

$$s = \{s_1 \; s_2 \; \cdots \; s_p \; s_{p+1} \; s_{p+2} \; \cdots \; s_{p+q}\}^T$$

$$= \{a_1 \; a_2 \; \cdots \; a_p \; b_1 \; b_2 \; \cdots \; b_q\}^T \tag{13}$$

The structural members that caused the changes in the jth measured mode are to be located. The changes in the mode could be caused by damage at a single member or at multiple members. Assume, for the time being, that the damage is caused by a single member. To locate the damaged single member, the influence of the structural member damage corresponding to the kth reduction factor s_k ($k = 1, \ldots, p+q$) on the jth mode is examined. Consider the kth reduction factor to obtain the fundamental equation of the proposed damage location algorithm as

$$\boldsymbol{L}_{kj}\gamma_{kj} = \phi_{tj} \tag{14}$$

where

$$\boldsymbol{L}_{kj} = \begin{cases} \boldsymbol{A}_{kj} & \text{for } k = 1, \ldots, p \\ \boldsymbol{B}_{(k-p)j} & \text{for } k = p+1, \ldots, p+q \end{cases} \tag{15}$$

$$\gamma_{kj} = s_k\phi_{tj} \quad \text{for } k = 1, \ldots, p+q \tag{16}$$

The implication of Eq. (14) is of significant importance. Equation (14) can only be true if the measured mode ϕ_{tj} is a linear combination of the columns of $\boldsymbol{L}_{kj}$. That is, ϕ_{tj} must lie in the subspace spanned by the columns of $\boldsymbol{L}_{kj}$. The implication of this statement is that, if damage has been caused by the loss of stiffness or mass in element k and this damage is reflected in mode j (i.e., mode j is different from the undamaged mode j), then the vector ϕ_{tj} will lie precisely in the subspace spanned by the columns of $\boldsymbol{L}_{kj}$. If, on the other hand, damage is caused by an element other than element k or this damage is not reflected in mode j, ϕ_{tj} would not lie in the subspace spanned by the columns of $\boldsymbol{L}_{kj}$.

To evaluate whether or not the measured mode lies in the subspace spanned by the columns of $\boldsymbol{L}_{kj}$, we turn to the concept of the best achievable eigenvectors[12] which is used in the eigenstructure assignment techniques. A new vector, which is as close as possible to ϕ_{tj}, can be computed as the projection of the measured mode onto the subspace spanned by the nonzero columns of $\boldsymbol{L}_{kj}$ as follows[12]

$$\phi^a_{kj} = \hat{\boldsymbol{L}}_{kj}\hat{\boldsymbol{L}}^+_{kj}\phi_{tj} \tag{17}$$

where $\hat{\boldsymbol{L}}_{kj}$ is the matrix $\boldsymbol{L}_{kj}$ where the zero columns have been removed to enhance computational efficiency, and the superscript + indicates the pseudoinverse of a matrix. The vector ϕ^a_{kj} is defined as the best achievable eigenvector for structural element k and mode j and the matrix product provides an alternative means of computing the subspace rotation as discussed in Ref. 15. The main difference is that the method in Ref. 15 identifies those DOFs that are affected by damage, whereas the method in this paper identifies directly the structural element that is damaged. Hence, the proposed method avoids the additional step of identifying damaged structural members from the affected DOF information due to damage, which can be cumbersome at times.

If the measured vector ϕ_{tj} already lies in the subspace, then ϕ^a_{kj} and ϕ_{tj} will be identical. If the damage is caused by a different element or the damage is not reflected in mode j, the two vectors will be different. If ϕ^a_{kj} is computed for all elements that could possibly have caused the damage and the Euclidean distance between these vectors and the corresponding measured modes is computed, the damaged element will be indicated by (in the case of perfect data) zero distance between the two vectors. All others will have nonzero values. The distance between the two vectors can be computed using the Frobenious norm

$$d_{kj} = \left\| \phi_{tj} - \phi^a_{kj} \right\|_F \tag{18}$$

where $\|\cdot\|_F$ represents the Frobenious norm. For a structure that has e structural members that could possibly have caused the damage and r measured modes, an $e \times r$ matrix of d's can be constructed as

$$\boldsymbol{D} = \begin{bmatrix} d_{11} & d_{12} & \cdots & d_{1j} & \cdots & d_{1r} \\ \vdots & \vdots & & \vdots & & \vdots \\ d_{k1} & d_{k2} & \cdots & d_{kj} & \cdots & d_{kr} \\ \vdots & \vdots & & \vdots & & \vdots \\ d_{e1} & d_{e2} & \cdots & d_{ej} & \cdots & d_{er} \end{bmatrix} \tag{19}$$

If damage is located in element k and this damage affects only mode j significantly so that the change in the frequency is measurable, then d_{kj} will be equal or close to zero. All other coefficients will be populated with nonzero entries. Therefore, the location of damage can be identified by searching for a value that is considerably smaller than others in the matrix.

Determining the Magnitude of Damage

Once the damaged elements or a number of suspected elements have been identified from the examination described previously, the extent of the damage can be determined by solving for the reduction factors s_k. Assume that the magnitude of damage is to be examined for $\hat{p}$ number of stiffness elements and $\hat{q}$ number of mass elements with the r number of test modes. Equation (7) can be written with only those elements as

$$\sum_{i=1}^{\hat{p}} a_i\hat{\boldsymbol{A}}_i + \sum_{i=1}^{\hat{q}} b_i\hat{\boldsymbol{B}}_i = \boldsymbol{R} \tag{20}$$

where

$$\hat{\boldsymbol{A}}_i = \boldsymbol{K}_i\Phi_t \tag{21}$$

$$\hat{\boldsymbol{B}}_i = -\boldsymbol{M}_i\Phi_t\Lambda_t \tag{22}$$

$$\boldsymbol{R} = \boldsymbol{M}_u\Phi_t\Lambda_t - \boldsymbol{K}_u\Phi_t \tag{23}$$

Define a vector containing the reduction factors corresponding to the elements being examined as

$$\hat{\boldsymbol{s}} = \{a_1 \; a_2 \ldots a_{\hat{p}} \; b_1 \; b_2 \ldots b_{\hat{q}}\}^T \tag{24}$$

By equating each column of Eq. (20) and rearranging, we obtain

$$\hat{\boldsymbol{L}}\hat{\boldsymbol{s}} = \boldsymbol{r} \tag{25}$$

where

$$\hat{\boldsymbol{L}} = \begin{bmatrix} \hat{\boldsymbol{A}}_{11} & \hat{\boldsymbol{A}}_{21} & \ldots & \hat{\boldsymbol{A}}_{\hat{p}1} & \hat{\boldsymbol{B}}_{11} & \hat{\boldsymbol{B}}_{21} & \ldots & \hat{\boldsymbol{B}}_{\hat{q}1} \\ \hat{\boldsymbol{A}}_{12} & \hat{\boldsymbol{A}}_{22} & \ldots & \hat{\boldsymbol{A}}_{\hat{p}2} & \hat{\boldsymbol{B}}_{12} & \hat{\boldsymbol{B}}_{22} & \ldots & \hat{\boldsymbol{B}}_{\hat{q}2} \\ \vdots & \vdots & \cdots & \vdots & \vdots & \vdots & \cdots & \vdots \\ \vdots & \vdots & \cdots & \vdots & \vdots & \vdots & \cdots & \vdots \\ \hat{\boldsymbol{A}}_{1r} & \hat{\boldsymbol{A}}_{2r} & \ldots & \hat{\boldsymbol{A}}_{\hat{p}r} & \hat{\boldsymbol{B}}_{1r} & \hat{\boldsymbol{B}}_{2r} & \ldots & \hat{\boldsymbol{B}}_{\hat{q}r} \end{bmatrix} \tag{26}$$

$$\boldsymbol{r} = \{\boldsymbol{R}_1^T \; \boldsymbol{R}_2^T \ldots \boldsymbol{R}_r^T\}^T \tag{27}$$

The vectors $\hat{\boldsymbol{A}}_{ij}$ and $\hat{\boldsymbol{B}}_{ij}$ represent the jth columns of matrices $\hat{\boldsymbol{A}}_i$ and $\hat{\boldsymbol{B}}_i$, respectively. The vector $\boldsymbol{R}_j$ is the jth column of the matrix $\boldsymbol{R}$. The sizes of $\hat{\boldsymbol{L}}$ and $\boldsymbol{R}$ are $nr \times (\hat{p}+\hat{q})$ and $nr \times 1$, respectively. The reduction factors in Eq. (25) can be solved using a pseudoinverse solution as

$$\hat{\boldsymbol{s}} = \hat{\boldsymbol{L}}^+\boldsymbol{r} \tag{28}$$

An accurate solution to the preceding equation is obtained when $nr \geq \hat{p} + \hat{q}$ and the matrix $\hat{\boldsymbol{L}}$ is of full rank, i.e., rank $(\hat{\boldsymbol{L}}) = \hat{p} + \hat{q}$. Therefore, whenever possible, the number of measured modes incorporated for the computation of the reduction factors must meet the condition as

$$r \geq \frac{\hat{p} + \hat{q}}{n} \tag{29}$$

Detection of Multiple Damage

When there is more than one damaged element in the structure, the examination of the matrices $\boldsymbol{D}$ in Eq. (19) may not provide a clear indication of the damaged members. If the matrix $\boldsymbol{D}$ does not indicate the damaged member clearly, it may imply that there are multiple damaged members. To examine multiple damage, a sequential damage detection approach is proposed. In this approach, damaged members are identified one at a time in an iterative process. The first step of the approach is to select the single most probable damaged member by examining the $\boldsymbol{D}$ matrix. Next, the magnitude of damage of the member is computed using Eq. (28). Then, the undamaged mass and/or stiffness matrices in Eq. (9) are modified to reflect the element mass and/or stiffness matrix changes corresponding to the member that has been located as damaged. For instance, if strut k has been identified as a damaged member and the corresponding stiffness reduction factor $a_k (-1 \leq a_k \leq 0)$ is computed, the undamaged stiffness matrix will be modified as

$$\boldsymbol{K}_u' = \boldsymbol{K}_u + a_k \boldsymbol{K}_k \tag{30}$$

where the matrix $\boldsymbol{K}_u'$ is the new undamaged stiffness matrix.

Then, the new undamaged mass and/or stiffness matrices are used to compute the new best achievable eigenvectors in Eq. (17) and a new $\boldsymbol{D}$ matrix in Eq. (19). Again, another single most probable damaged member is selected using the new $\boldsymbol{D}$ matrix. This iterative process is continued until all the damaged members are located. At the end of each iteration, the natural frequencies are computed using the new undamaged matrices and compared with those of measured frequencies. When the differences are small, i.e., within the usual error bound of a modal test, the iteration terminates. This comparison also can be used to ascertain whether the selected member is indeed responsible for the damage. The eight-bay truss example will illustrate how this approach is used to locate multiple damage.

Filtering of the Measured Mode Shapes

When the measured modes are accurate (i.e., free from noise, bias, measurement errors, and nonlinearity effects), the magnitude of damage can be obtained accurately using the measured modes directly as described previously. However, the measured modes are usually contaminated by noise, nonlinearity, and measurement errors. When these noisy measured modes are used directly to compute the magnitude of damage, unrealizable values of the reduction factors can be obtained, i.e., the values of the stiffness and mass reduction factors do not lie between 0 and −1. The concept of the best achievable vectors can be utilized to filter the measured mode shapes from the contamination.

Consider the $\hat{p}$ number of damaged stiffness element and $\hat{q}$ number of damaged mass element that have been identified with the r number of test modes. Then, Eq. (12) can be written as

$$\sum_{i=1}^{\hat{p}} a_i \boldsymbol{A}_{ij} \phi_{tj} + \sum_{i=1}^{\hat{q}} b_i \boldsymbol{B}_{ij} \phi_{tj} = \phi_{tj} \tag{31}$$

Define a vector

$$\tilde{\gamma}_j = \{a_1 \phi_{tj}^T \; a_2 \phi_{tj}^T \ldots a_{\hat{p}} \phi_{tj}^T \; b_1 \phi_{tj}^T \; b_2 \phi_{tj}^T \ldots b_{\hat{q}} \phi_{tj}^T\}^T \tag{32}$$

Then Eq. (31) can be rearranged as

$$\tilde{\boldsymbol{L}}_j \tilde{\gamma}_j = \phi_{tj} \tag{33}$$

where

$$\tilde{\boldsymbol{L}}_j = [\boldsymbol{A}_{1j} \; \boldsymbol{A}_{2j} \ldots \boldsymbol{A}_{\hat{p}j} \; \boldsymbol{B}_{1j} \; \boldsymbol{B}_{2j} \ldots \boldsymbol{B}_{\hat{q}j}] \tag{34}$$

Again, we see that the measured mode ϕ_{tj} must lie in the subspace spanned by the columns of $\tilde{\boldsymbol{L}}_j$. The best achievable eigenvector, which is as close as possible to ϕ_{tj}, can be computed as the projection of the measured mode onto the subspace spanned by the columns of $\tilde{\boldsymbol{L}}_j$ as follows

$$\phi_{tj}^f = \tilde{\boldsymbol{L}}_j \tilde{\boldsymbol{L}}_j^+ \phi_{tj} \tag{35}$$

The vector ϕ_{tj}^f is defined as the filtered eigenvector. Because the subspace defined by the matrix $\tilde{\boldsymbol{L}}_j$ contains the information on the analytical model and the measured frequencies, the information in the measured mode shape which is not compatible with the analytical model will be filtered out. The effectiveness of using the analytical model as a means to filter the test mode shapes depends on the degree of correlation of the analytical model to the test data of the undamaged structure.

Define a filtered test mode shape matrix

$$\boldsymbol{\Phi}_t^f = [\phi_{t1}^f \; \phi_{t2}^f \ldots \phi_{tr}^f] \tag{36}$$

Now the filtered mode shape matrix can be substituted in Eqs. (21–23) to solve for the reduction factors in Eq. (24). The effect of filtering the measured mode shapes will be examined using the eight-bay laboratory space truss structure example that follows.

Damage Detection of Laboratory Eight-Bay Space Truss

The cantilevered, eight-bay laboratory space truss structure shown in Fig. 1 is used as a damage location test bed at the NASA Langley Research Center. Each bay of the truss is a cube with the side dimension of 19.685 in. (0.5 m). Truss members (longerons, battens, and diagonals) are connected through interchangeable node balls. Detailed information on the test program and the test bed are available in Ref. 17.

Five damage cases listed in Table 1 were examined. In damage cases A through C, damage refers to the total removal of a single strut. In case D, a previously buckled strut was inserted in place of a longeron and damage case E has multiple member damage. Figure 2 shows the test configuration and the locations of struts that were removed for each of the cases. The truss was instrumented with three accelerometers at each node providing a full set of translational mode shapes. Typically, modal tests have limited sets of sensors and thus truncated mode shape vectors. Having a complete characterization of the mode shapes is a tremendous asset for this kind of work as it allows for a determination of the true effects of measurement noise on a particular algorithm. Modal tests were performed for the undamaged structure and each of the damage cases. To evaluate the performance of the proposed method with actual test data, analytical models were generated corresponding to the undamaged structure and each of the damage cases. Table 2 shows the variation in natural frequencies for the first five modes of the truss due to damage. Modes 1 and 2 are the first bending modes. Mode 3 is the first torsional mode. Modes 4 and 5 are the second bending modes.

Predetection Analysis

Assume that modal testing is performed to the truss structure periodically to monitor the health of the structure. The effort to detect damage will normally be initiated when there is a change in the test frequency which is greater than the usual error bound of the modal testing. This error bound may vary significantly depending on a particular modal testing environment. For this example, because the structure is placed in a controlled laboratory environment and the first five modes are considered, the error bound on the frequency is assumed to be about ±2%. Damage detection effort will normally be initiated only if there is a frequency change

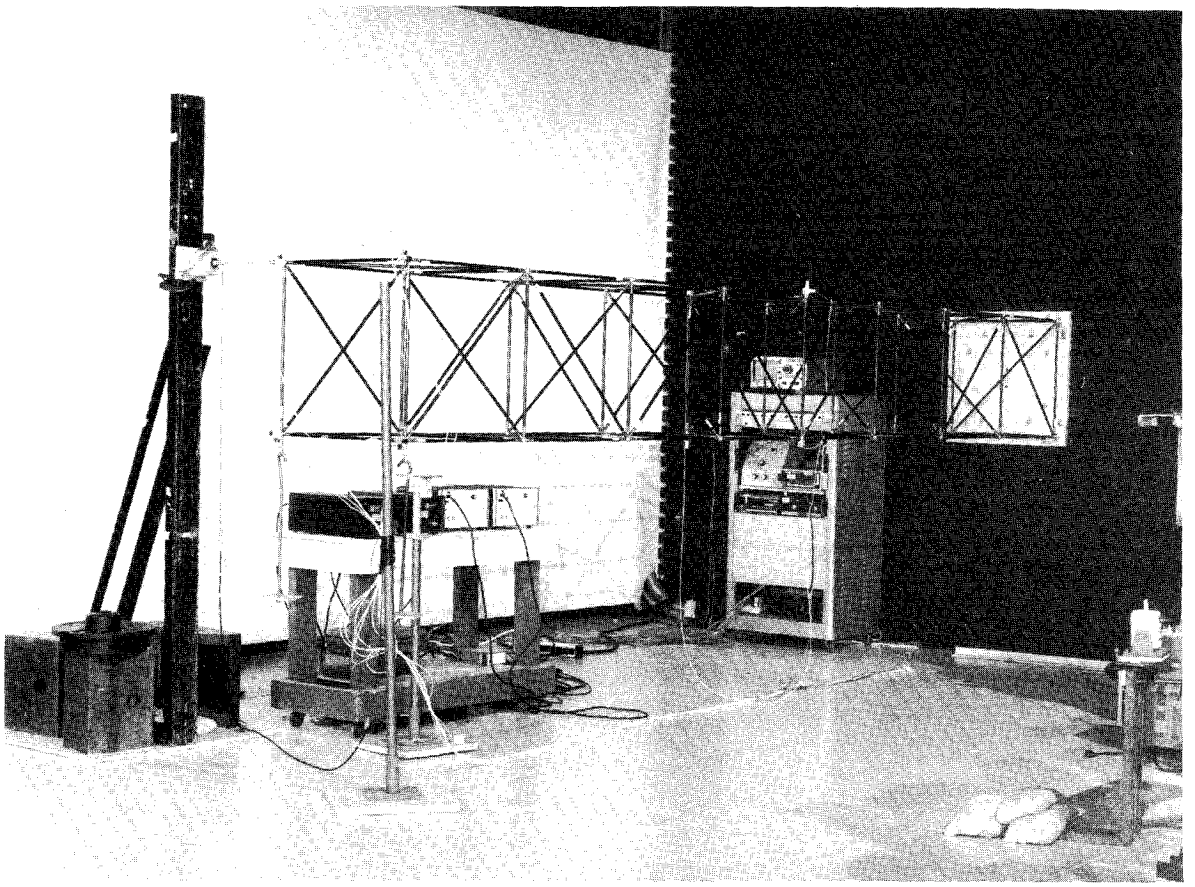

Fig. 1 Eight-bay space truss test structure.

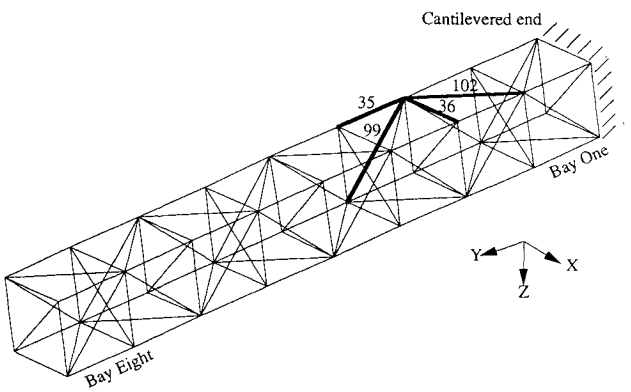

Fig. 2 Eight-bay truss damaged strut locations.

greater than the error bound among the first five modes. Under this criterion, the damage cases B and D will be regarded as if there is no damage even though damage exists. This is the inherent shortcoming of the damage detection approach using the measured modes.

As was pointed out in Ref. 2, all 104 struts in the truss structure cannot be monitored for damage because only the first five modes are available and the measured modes contain errors. Using the modal strain energy (MSE) information, the members for which damage detection is feasible can be identified. The MSE for strut i and mode j is defined as

$$\mathrm{MSE}_{ij}(\%) = \frac{\phi_j^T \boldsymbol{K}_i \phi_j}{\omega_j^2} \times 100 \tag{37}$$

Table 1 Damage cases investigated for the eight-bay truss

Damage case	Damaged strut number	Damage condition
A	35 (Longeron)	Strut out
B	36 (Batten)	Strut out
C	102 (Diagonal)	Strut out
D	35 (Longeron)	Buckled strut
E	35 (Longeron) and 99 (Diagonal)	Strut out

Considering each strut one at a time, the percent MSE contained in a strut for a mode is approximately equivalent to the same percent frequency change for that mode when the strut is damaged completely. For instance, if a strut contains 2% MSE for a mode, the removal of the strut would bring about 2% frequency change for the mode. As the frequency measurement error bound is assumed at 2%, damage detection for the struts containing less than 2% MSE will be difficult if not impossible. Also, from the numerical conditioning perspective, the matrix $\boldsymbol{E}_j$ in Eq. (9) can be ill-conditioned if a test mode corresponding to frequency change much less than 2% is used for damage detection.

In this example, to be conservative, all struts that have more than 1% MSE are included as candidates for damage detection. Table 3 shows the MSE distribution among the first five modes. All the struts that have more than 1% MSE contribution for each mode are listed. There are 50 struts containing more than 1% MSE among the 104 struts. Strut 36 (batten) does not have strain energy over 1% among the first five modes. Therefore, among the damage cases shown in Table 1, the damage case B corresponding to strut 36 damage is considered undetectable for practical purposes.

Damage Detection

The best achievable eigenvectors are computed for the struts which contain over 1% of modal strain energy for each of the first

five modes. Simulated test modes and actual laboratory test modes are both used to compute the detection matrix $\boldsymbol{D}$ in Eq. (19). Tables 4 and 5 show the resulting Euclidean distances for damage case A. Modes 2 and 5 are used in this case because they bring significant natural frequency changes as shown in Table 2. For each mode, only those struts that have more than 1% MSE were included in the examination. By showing zero distance between the analysis mode shape and the best achievable eigenvector, simulated analysis data clearly indicate the damage location, strut 35, for both modes 2 and 5. However, examination of the Euclidean distances obtained using actual test data shown in Tables 4 and 5 indicates that there are possibilities of damage at strut 35, strut 27, or both strut 35 and 37 because the distances at these locations are consistently smaller than the others. Determination of the damaged member(s) will not be made until the damage magnitudes are computed for the suspicious damaged struts. As will be seen more for other damage cases, a situation like this occurs frequently when actual test data is used for damage detection.

To determine the damaged strut(s) for damage case A when the actual test data is used, the following procedure is employed. Assuming that either strut 35 or strut 27 is damaged, the magnitude of damage is computed for strut 35 and strut 27 independently using Eq. (28). The element stiffness matrix corresponding to the damaged strut and modes 2 and 5 are incorporated to compute the magnitude. The resulting magnitudes of damage are as follows: −1.00 for strut 35 and 18.29 for strut 27. This indicates that the damage occurred at strut 35 and the magnitude is −1, i.e., complete loss of stiffness. The analytical model modified to reflect the damage at strut 35 closely produces the test frequencies for damage case A shown in Table 2. Thus, the damage detection process is completed.

Simulated and filtered modes are also employed independently to evaluate the magnitude of damage at strut 35. The filtered modes are obtained using Eq. (35) along with the element stiffness matrix corresponding to strut 35. The resulting magnitudes of damage are included in Table 6 along with other damage cases. Simulated modes produce the exact damage magnitude. Filtered modes also produce accurate damage magnitude.

As discussed previously, damage case B is considered undetectable because it does not produce enough natural frequency

Table 2 Natural frequency variation due to damage (Hz)

	Mode 1		Mode 2		Mode 3		Mode 4		Mode 5	
Damage cases	Anal.	Test	Anal.	Test	Anal	Anal.	Anal	Anal.	Anal	Anal.
Undamaged	13.92	13.88	14.44	14.48	46.74	48.41	66.01	64.03	71.14	67.46
A	13.92	13.97	11.35	11.39	46.74	48.53	66.01	64.50	61.04	59.90
	(0.00)[a]	(0.65)	(−21.4)	(−21.3)	(0.00)	(0.25)	(0.00)	(0.73)	(−14.2)	(−11.2)
B	13.92	13.90	14.44	14.52	46.74	48.53	65.90	64.31	71.05	67.54
	(0.00)	(0.14)	(0.00)	(0.28)	(0.00)	(0.25)	(−0.17)	(0.44)	(−0.13)	(0.12)
C	13.27	13.47	14.24	14.12	33.44	35.65	60.39	60.18	68.87	65.86
	(−4.67)	(−2.95)	(−1.39)	(−2.49)	(−28.5)	(−26.4)	(−8.51)	(−6.01)	(−3.19)	(−2.37)
D	N/A	13.83	N/A	14.24	N/A	48.43	N/A	64.03	N/A	66.42
		(−0.36)		(−1.66)		(0.04)		(0.00)		(−1.54)
E	13.65	13.74	9.77	9.86	34.68	36.66	64.32	63.35	59.66	58.86
	(−1.94)	(−1.01)	(−32.3)	(−31.9)	(−25.8)	(−24.3)	(−2.56)	(−1.06)	(−16.1)	(−12.7)

[a]Numbers in parentheses indicate percent frequency changes with respect to the undamaged analytical and test frequencies.

Table 3 Percent modal strain energy distribution among the first five modes[2]

	Mode number						Mode number				
Strut ID	1	2	3	4	5	Strut ID	1	2	3	4	5
9	-[a]	-	-	3.0	-	49	21.0	-	-	8.2	-
10	-	-	-	3.0	-	86	-	-	1.5	-	-
15	-	1.2	-	-	7.4	87	-	-	1.5	-	-
16	-	1.2	-	-	7.4	88	-	-	1.5	-	-
17	-	-	-	3.3	-	89	-	-	1.5	-	-
19	-	-	6.0	3.3	-	90	-	-	2.6	-	-
21	2.7	-	-	8.2	-	91	-	-	2.6	-	-
22	2.7	-	-	8.2	-	92	-	-	2.6	-	-
23	-	1.2	-	-	7.7	93	-	-	2.6	-	-
25	-	1.2	-	-	7.7	94	-	-	3.7	-	-
27	-	5.9	-	-	4.8	95	-	-	3.7	-	-
28	-	5.9	-	-	4.8	96	-	-	3.7	-	-
29	2.7	-	-	8.3	-	97	-	-	3.7	-	-
31	2.7	-	-	8.3	-	98	-	-	4.8	1.1	1.6
33	9.4	-	-	1.2	-	99	-	-	4.8	1.1	1.6
34	9.4	-	-	1.2	-	100	-	-	4.8	1.1	1.6
35	-	5.9	-	-	4.8	101	-	-	4.8	1.1	1.6
37	-	5.9	-	-	4.8	102	-	-	5.5	2.4	3.0
39	-	15.7	-	-	1.9	103	-	-	5.5	2.4	3.0
40	-	15.7	-	-	1.9	104	-	-	5.5	2.4	3.0
41	9.4	-	-	1.2	-	105	-	-	5.5	2.4	3.0
43	9.4	-	-	1.2	-	106	-	-	6.0	3.2	3.5
45	-	15.7	-	-	2.0	107	-	-	6.0	3.2	3.5
46	-	15.7	-	-	2.0	108	-	-	6.0	3.2	3.5
47	21.0	-	-	8.2	-	109	-	-	-	3.2	3.5

[a]"-" indicates that the MSE contribution is less than 1%.

changes. Damage case C produces significant natural frequency changes for all five modes. The two largest frequency changes occur at modes 3 and 4. Thus, modes 3 and 4 will be used to examine the damage. Tables 7 and 8 show the Euclidean distances computed using simulated analysis modes and test modes. The damaged strut is clearly located using analysis modes. Unlike case A, the test modes also clearly indicate a single location of damage, strut 102. As the location of the damage is identified, modes 3 and 4 are used to compute the magnitude for damage case C along with the element stiffness matrix corresponding to strut 102. Accurate damage magnitudes are obtained regardless of whether simulated, test, or filtered modes are used as summarized in Table 6.

Case D, the buckled strut case, shows marginal frequency changes for modes 2 and 5. As discussed previously, the changes in natural frequencies of less than 2% measurement error bound will not be sufficient to initiate the damage detection process. However, damage detection will be attempted here to show the im-

Table 4 Results of damage case A using mode 2

	Euclidean distances	
Strut ID	Simulated data	Test data
15	6.01	6.22
16	6.62	6.85
23	5.99	6.15
25	6.85	7.03
27	1.25	2.91
28	2.79	3.82
35	**0.00**	**2.58**
37	2.91	3.88
39	3.58	4.60
40	4.19	5.08
45	4.24	5.12
46	3.65	4.64

Table 5 Results of damage case A using mode 5

	Euclidean distances	
Strut ID	Simulated data	Test data
15	9.92	11.14
16	13.04	13.91
23	9.30	10.61
25	13.50	14.30
27	4.63	6.71
28	13.02	13.77
35	**0.00**	**5.25**
37	13.64	14.54
39	19.45	20.67
40	11.74	14.22
45	12.23	14.62
46	19.63	20.81
98	29.70	31.16
99	29.70	28.03
100	29.54	28.41
101	29.54	30.69
102	29.58	31.01
103	29.73	28.14
104	29.58	27.40
105	29.73	30.80
106	29.89	28.22
107	29.89	30.95
108	30.09	31.41
109	30.09	27.98

Table 6 Summary of damage detection results for the eight-bay truss

		Damage magnitudes obtained using		
Damage case	Damaged struts located	Simulated modes	Test modes	Filtered modes
A	35	−1.00	−1.00	−1.02
B	Unable to be located	-	-	-
C	102	−1.00	−1.01	−0.99
D	Unable to be located	-	-	-
E	35 and 99	−1.00 and −1.00	−0.96 and −0.99	−0.99 and −0.99

Table 7 Results of damage case C using mode 3

	Euclidean distances	
Strut ID	Simulated data	Test data
19	32.67	32.72
86	25.28	23.82
87	22.69	21.07
88	23.20	21.12
89	19.86	17.80
90	20.73	19.44
91	20.71	19.34
92	20.03	18.45
93	20.10	18.27
94	15.74	14.79
95	19.14	17.60
96	19.51	18.18
97	21.93	20.28
98	10.73	10.47
99	19.30	18.31
100	18.92	17.50
101	24.17	22.58
102	**0.00**	**3.09**
103	19.51	18.13
104	19.60	18.55
105	25.87	24.33
106	20.83	19.44
107	26.66	25.13
108	9.92	9.62

Table 8 Results of damage case C using mode 4

	Euclidean distances	
Strut ID	Simulated data	Test data
9	22.11	22.92
10	22.02	22.91
17	22.17	22.96
19	22.03	22.93
21	21.63	22.53
22	21.51	22.52
29	21.65	22.57
31	21.51	22.51
33	22.92	23.87
34	22.54	23.64
41	23.08	24.03
43	22.70	23.80
47	21.41	22.37
49	21.57	22.46
98	8.63	8.41
99	28.23	27.44
100	33.21	33.43
101	27.98	29.80
102	**0.00**	**3.32**
103	32.78	33.12
104	27.91	27.29
105	25.66	27.76
106	32.51	32.89
107	25.10	27.23
108	6.44	7.70
109	27.76	27.24

Table 9 Results of damage case D

Strut ID	Test data: mode 2	Strut ID	Test data: mode 5	Strut ID	Test data: mode 5
15	19.91	15	8.22	98	33.25
16	19.91	16	8.60	99	31.71
23	19.91	23	8.22	100	31.71
25	19.91	25	8.68	101	33.25
27	19.91	27	8.03	102	33.22
28	19.91	28	8.80	103	31.81
35	19.91	35	8.13	104	31.80
37	19.91	37	9.08	105	33.22
39	19.91	39	11.12	106	31.87
40	19.91	40	10.02	107	33.19
45	19.91	45	10.21	108	33.19
46	19.91	46	11.25	109	31.87

Table 10 Results of damage case E using mode 2

	Euclidean distances		Euclidean distances[a]	
Strut ID	Analysis data	Test data	Analysis data	Test data
15	12.18	12.42	7.47	7.47
16	12.71	13.06	15.24	15.54
23	12.21	12.42	7.48	7.46
25	12.94	13.25	15.42	15.69
27	8.35	9.29	1.39	3.01
28	8.98	9.87	14.31	14.98
35	8.24	9.16	**0.00**	**2.60**
37	9.05	9.91	14.34	15.00
39	8.45	9.50	9.55	10.48
40	8.93	9.93	5.05	6.08
45	8.97	9.96	5.11	6.13
46	8.51	9.55	9.60	10.53

[a]Obtained after the damage at strut 99 has been detected.

pact of measurement error. Because the stiffness loss due to buckling is not predictable, analytical modes are not available. Only test modes are used to detect the damage location. Table 9 shows the Euclidean distances using modes 2 and 5. It is impossible to locate the strut that caused the damage as expected.

Tables 10–12 show the damage detection results for case E, the multiple damage case. Modes 2, 3, and 5 are employed because they undergo significant changes as indicated in Table 5. Euclidean distances are computed using these modes and shown in columns 2 and 3. Even though strut 35 shows the smallest distance for modes 2 and 5, the magnitude is too large to draw a conclusion that strut 35 is the damaged member. The distance corresponding to strut 99, computed using modes 3 and 5, provides conflicting information. The distance obtained using mode 3 convincingly indicates that strut 99 is the damaged member whereas the distance obtained using mode 5 implies the opposite. One conclusion that may be drawn from this seemingly contradicting information is that there is more than a single damaged strut and that strut 99 is most likely to be one of them. As mode 3 clearly indicates damage at strut 99, the damage magnitude is computed for strut 99 using mode 3 and the element stiffness matrix corresponding to the strut. The resulting magnitudes are −1.03 and −1.01 for analytical and test modes, respectively, and they indicate complete damage at strut 99. The natural frequencies computed reflecting complete damage at strut 99 still contain large errors even though they have been improved.

To locate the rest of the damaged members, the undamaged stiffness matrix in Eq. (9) is modified to reflect the damage at strut 99 using Eq. (30) with $k = 99$ and $a_k = -1$. The modified stiffness matrix is then treated as the new undamaged stiffness matrix to compute the Euclidean distances. The results are shown in the last two columns of Tables 10–12. Now strut 35 is clearly identified as the damaged member using modes 2 and 5. The magnitudes of damage are computed for struts 35 and 99 with simulated, test, and

Table 11 Results of damage case E using mode 3

	Euclidean distances		Euclidean distances[a]	
Strut ID	Analysis data	Test data	Analysis data	Test data
19	32.87	32.94	1.72	23.08
86	20.84	18.84	1.33	8.95
87	17.97	15.59	1.27	4.99
88	22.55	20.52	1.17	10.08
89	19.95	17.96	1.13	9.47
90	17.96	16.13	1.29	8.17
91	16.96	15.73	1.18	5.83
92	17.64	15.46	1.24	4.81
93	16.96	15.19	1.17	8.31
94	16.21	14.51	1.21	6.64
95	19.60	17.51	1.23	5.69
96	11.27	10.24	1.21	4.66
97	15.80	14.24	1.21	6.53
98	16.28	14.72	1.20	4.18
99	**1.23**	**3.25**	-	-
100	21.65	19.62	2.91	28.12
101	16.18	14.69	1.24	3.92
102	17.87	16.34	1.15	7.18
103	22.80	20.87	1.19	7.43
104	10.39	9.84	1.26	3.85
105	18.09	16.63	1.28	6.62
106	23.61	21.75	1.18	7.58
107	19.76	18.16	1.31	7.63
108	19.55	18.04	1.17	8.05

[a]Obtained after the damage at strut 99 has been detected.

Table 12 Results of damage case E using mode 5

	Euclidean distances		Euclidean distances[a]	
Strut ID	Analysis data	Test data	Analysis data	Test data
15	15.61	17.85	8.32	8.53
16	17.24	19.19	11.29	10.30
23	15.32	17.63	7.88	8.10
25	17.51	19.38	11.56	10.56
27	13.68	16.31	3.79	7.00
28	17.27	19.13	13.07	10.79
35	13.03	15.93	**0.00**	**6.03**
37	17.69	19.58	13.30	11.20
39	22.03	23.64	25.99	28.02
40	17.57	20.12	9.72	10.77
45	17.92	20.39	9.99	11.10
46	22.24	23.79	26.13	28.09
98	33.13	33.20	28.80	30.11
99	21.81	20.08	-	-
100	29.32	30.36	20.37	18.05
101	30.83	30.77	32.91	32.98
102	33.05	33.21	15.28	18.94
103	28.46	29.28	20.75	18.73
104	21.76	19.58	21.92	20.05
105	31.38	31.37	30.35	30.15
106	28.33	29.02	20.92	18.93
107	31.64	31.67	30.37	30.16
108	33.11	33.21	18.15	21.39
109	22.97	20.84	23.14	21.60

[a]Obtained after the damage at strut 99 has been detected.

filtered modes and shown in Table 6. The filtered modes are obtained using element stiffness matrices corresponding to struts 35 and 99. Natural frequencies obtained using the damage at struts 35 and 99 predict the test frequencies accurately. Struts 35 and 99 are thus confirmed to be the damaged members.

Concluding Remarks

A new damage detection method has been developed based on the best achievable eigenvector concept that has been used in the

controls community to design control systems. The best achievable eigenvector is a projection of a measured mode shape onto the subspace that is defined by the undamaged analytical model and measured natural frequencies. The Euclidean distance between the measured mode shape and the best achievable eigenvector is then used to locate the damage. Once the damage is located, the magnitude of damage is computed using an efficient least squares solution. Instead of identifying the mass or stiffness matrix coefficients, the method directly locates the damaged structural member thanks to the incorporation of element mass and stiffness matrices. Thus the extra step of identifying the structural member from the matrix coefficient changes is eliminated. The exact location and magnitude of damage can be obtained when simulated test data are used. As was shown in the eight-bay truss structure, the method also performs well when experimentally obtained modes are used. Multiple damage can also be detected using a sequential damage detection approach.

Because a limited number of noisy measured modes is typically available for damage location, it is unrealistic to expect that any damage in the structure will be detected. A predetection analysis is proposed using modal strain energy (MSE) with a given accuracy of measured modes. Damage detection of a structural element whose MSE is below a threshold value is considered infeasible. The threshold value would depend on the accuracy of modal test data. The predetection analysis is a process of incorporating the inherent limitations of the damage detection approaches that employ a finite number of noisy measured modes and system identification methods. However, using this type of specified value of MSE to establish damage detection feasibility may have a shortcoming. A likely damage scenario is one in which damage occurs to several structural members which individually have MSE values less than the threshold value but whose collective damage causes appreciable changes in modes. In this case, damage detection will not be feasible for the members as they are not in the candidate list. When this happens, it will become necessary to include all the structural members in the candidate list.

When the measured modes are extremely noisy, the magnitude of damage may become unrealistic, i.e., exceed the meaningful bounds of the stiffness reduction factor. The measured modes can be filtered through the analytical model and the measured frequency. This filtering process eliminates the noise in the measured modes which is not consistent with the analytical model and thus unrealistic damage magnitudes can be avoided.

One significant aspect of the eight-bay truss example is that the mode shapes are available for the entire translational DOFs, which is very rare in a typical modal test. Thus, the influence of insufficient mode shapes on the damage detection is not addressed in this study. Future work should address the impact of not having a full set of mode shapes on the damage detection and how to select a given number of test DOFs to provide the best damage detection capability.

References

[1]Kashangaki, T., "On-Orbit Damage Detection and Health Monitoring of Large Space Trusses—Status and Critical Issues," *Proceedings of the AIAA/ASME/ASCE/AHS/ASC 32nd Structures, Structural Dynamics, and Materials Conference*, AIAA, Washington, DC, 1991, pp. 2947–2958 (AIAA Paper 91-1181).

[2]Kashangaki, T., Smith, S. W., and Lim, T. W, "Underlying Modal Data Issues for Detecting Damage in Truss Structures," *Proceedings of the AIAA/ASME/ASCE/AHS/ASC 33rd Structures, Structural Dynamics, and Materials Conference*, AIAA, Washington, DC, 1992, pp. 1437–1446 (AIAA Paper 92-2264).

[3]Brock, J. E., "Optimal Matrices Describing Linear Systems," *AIAA Journal*, Vol. 6, No. 7, 1968, pp. 1292–1296.

[4]Baruch, M., "Optimal Correction of Mass and Stiffness Matrices Using Measured Modes," *AIAA Journal*, Vol. 20, No. 11, 1982, pp. 1623–1626.

[5]Berman, A., and Nagy, E. J., "Improvement of a Large Analytical Model Using Test Data," *AIAA Journal*, Vol. 21, No. 8, 1983, pp. 1168–1173.

[6]Kabe, A. M., "Stiffness Matrix Adjustment Using Mode Data," *AIAA Journal*, Vol. 23, No. 9, 1985, pp. 1431–1436.

[7]Smith, S. W., and Hendricks, S. L., "Damage Detection and Location in Large Space Trusses," *AIAA SDM Issues of the International Space Station, A Collection of Technical Papers*, AIAA, Washington, DC, 1988, pp. 56–63.

[8]Kammer, D. C., "Optimum Approximation for Residual Stiffness in Linear System Identification," *AIAA Journal*, Vol. 26, No. 1, 1988, pp. 104–112.

[9]Smith, S. W., and Beattie, C. A., "Secant-Method Matrix Adjustment for Structural Models," *AIAA Journal*, Vol. 29, No. 1, 1991, pp. 119–126.

[10]Collins, J. D., Hart, G. C., Hasselman, T. K., and Kennedy, B., "Statistical Identification of Structures," *AIAA Journal*, Vol. 12, No. 2, 1974, pp. 185–190.

[11]Anon., *MSC/NASTRAN User's Manual*, Version 66, Macneal-Schwendler Corp., Los Angeles, CA, 1989.

[12]Andry, A. N., Shapiro, E. Y., and Chung, J. C., "Eigenstructure Assignment for Linear Systems," *IEEE Transactions on Aerospace and Electronic Systems*, Vol. AES-19, No. 5, 1983, pp. 711–729.

[13]Minas, C., and Inman, D. J., "Matching Finite Element Models to Modal Data," *Journal of Vibration and Acoustics*, Vol. 112, No. 1, 1990, pp. 84–92.

[14]Zimmerman, D. C., and Widengren, W., "Correcting Finite Element Models Using a Symmetric Eigenstructure Assignment Technique," *AIAA Journal*, Vol. 28, No. 9, 1990, pp. 1670–1676.

[15]Zimmerman, D. C., and Kaouk, M., "Structural Damage Detection Using a Subspace Rotation Algorithm," *Proceedings of the AIAA/ASME/ASCE/AHS/ASC 33rd Structures, Structural Dynamics, and Materials Conference*, AIAA, Washington, DC, 1992, pp. 2341–2350 (AIAA Paper 92-2521).

[16]Smith, S. W., and Beattie, C. A., "Simultaneous Expansion and Orthogonalization of Measured Modes for Structure Identification," *Proceedings of the AIAA Dynamics Specialist Conference*, AIAA, Washington, DC, 1990, pp. 261–270.

[17]Kashangaki, T., "Ground Vibration Tests of a High Fidelity Truss for Verification of On-Orbit Damage Location Techniques," NASA TM-107–26, May 1992.